Dual-colored graphene quantum dots-labeled nanoprobes/graphene oxide: functional carbon materials for respective and simultaneous detection of DNA and thrombin

2014 Nanotechnology 25 415501

(http://iopscience.iop.org/0957-4484/25/41/415501)

IOP Publishing Nanotechnology
Nanotechnology **25** (2014) 415501 (10pp) doi:10.1088/0957-4484/25/41/415501

Dual-colored graphene quantum dots-labeled nanoprobes/graphene oxide: functional carbon materials for respective and simultaneous detection of DNA and thrombin

Zhao Sheng Qian, Xiao Yue Shan, Lu Jing Chai, Jian Rong Chen and Hui Feng

College of Chemistry and Life Science, Zhejiang Normal University, Jinhua 321004, People's Republic of China

E-mail: fenghui@zjnu.cn

Received 4 July 2014
Accepted for publication 12 August 2014
Published 24 September 2014

Abstract

Convenient and simultaneous detection of multiple biomarkers such as DNA and proteins with biocompatible materials and good analytical performance still remains a challenge. Herein, we report the respective and simultaneous detection of DNA and bovine α-thrombin (thrombin) entirely based on biocompatible carbon materials through a specially designed fluorescence on-off-on process. Colorful fluorescence, high emission efficiency, good photostability and excellent compatibility enables graphene quantum dots (GQDs) as the best choice for fluorophores in bioprobes, and thus two-colored GQDs as labeling fluorophores were chemically bonded with specific oligonucleotide sequence and aptamer to prepare two probes targeting the DNA and thrombin, respectively. Each probe can be assembled on the graphene oxide (GO) platform spontaneously by π–π stacking and electrostatic attraction; as a result, fast electron transfer in the assembly efficiently quenches the fluorescence of probe. The presence of DNA or thrombin can trigger the self-recognition between capturing a nucleotide sequence and its target DNA or between thrombin and its aptamer due to their specific hybridization and duplex DNA structures or the formation of apatamer–substrate complex, which is taken advantage of in order to achieve a separate quantitative analysis of DNA and thrombin. A dual-functional biosensor for simultaneous detection of DNA and thrombin was also constructed by self-assembly of two probes with distinct colors and GO platform, and was further evaluated with the presence of various concentrations of DNA and thrombin. Both biosensors serving as a general detection model for multiple species exhibit outstanding analytical performance, and are expected to be applied *in vivo* because of the excellent biocompatibility of their used materials.

S Online supplementary data available from stacks.iop.org/NANO/25/415501/mmedia

Keywords: graphene quantum dots, graphene oxide, nanosensor, DNA detection, thrombin detection

(Some figures may appear in colour only in the online journal)

1. Introduction

The presence and quantity of biomarkers such as DNA, proteins and carbohydrates are usually regarded as important signals of specific disease states and physiological processes. This has been a distinctive advantage in accurate and sensitive early warning and diagnosis [1]. Therefore it is critical to discover novel and efficient detection strategies for these biomolecules, especially for simultaneous detection of multiplex species in a complex system. Furthermore, the safety and biocompatibility of the used materials are also of great significance for further application of constructed biosensors in cellular tissue or *in vivo* [2].

Several nanosensors have been built to achieve separate or simultaneous detection of different targets. Yang *et al* [3] utilized the assembly of single-walled carbon nanotubes (SWCNTs) and dye-labeled single-stranded DNA to develop a new class of fluorescent biosensors which are able to probe DNA and thrombin separately. Chen *et al* [4] adopted multi-walled carbon nanotubes (MWCNTs) and three dye-functionalized DNA probes to realize respective analysis of three DNA targets. He *et al* [5] reported a graphene oxide (GO)-based multicolor fluorescent DNA nanoprobe with different dyes as fluorophores that allows rapid and sensitive detection of multiplex DNA targets. Using a similar strategy based on GO and dye-labeled probes, Zhang *et al* [6] achieved respective sensing for multiplex targets including DNA, protein and small molecules. Li *et al* [7] constructed a multicolor fluorescent nanoprobe using three dye-terminated DNA sequences as reporters for detection and imaging of tumor-related mRNAs in living cells. These prior works focused on respective detection of multiplex targets or species with dye-labeled probes. However, organic dyes as fluorophores in the probes have non-negligible disadvantages including poor photostability, easy photobleaching and small Stokes shifts. For this reason, Mei *et al* [8] proposed a GO nanosheet–based assay for different biological species using silver nanoparticles (AgNPs) instead of dyes, which are functionalized with ligands, antibodies, and oligonucleotides. Liu *et al* [9] applied the tunable fluorescence of AgNPs to the multiplex analysis of DNAs and infectious pathogens. These reports demonstrated separate detection of several targets through design and construction of corresponding probes. To further establish more convenient and efficient biosensors for simultaneous detection of multiple species on the same platform, Chen *et al* [10] assembled two quantum dot (QD)–functionalized probes on GO at one time to realize simultaneous determination of human enterovirus 71 and coxsackievirus B3. Zhang *et al* [11] developed a novel detection strategy for multiplex lectins by labeling glucosamine and galactosamine with different-colored semiconductor QDs. Nevertheless, the drawbacks of semiconductor QDs [12] and AgNPs [13], such as high toxicity, relatively high cost and hard manipulation, still do not qualify them as excellent fluorophores of probes for biomolecules, which prompts scientists to investigate and exploit alternative fluorescent materials with good biocompatibility.

Since their discovery, graphene quantum dots (GQDs) have attracted the widespread attention of scientists in different fields because of their distinctive optical properties and outstanding performance in photovoltaic devices, photocatalysis and biological imaging [14–16]. Compared with the conventional dye molecules and semiconductor QDs, GQDs have many advantages such as stable light emitting, high quantum yield, good photostability, easy modulation, low toxicity and excellent biocompatibility. GQDs are expected to be the most promising environmentally friendly and biocompatible nanomaterial that can be used to design new fluorescence detection platforms *in vitro* and *in vivo*. In our previous work, we synthesized several modified GQDs with a small amount of organic compound and revealed the significant role of protonation of amino groups in the improvement of their fluorescence performance [17]. Furthermore, a series of heteroatom doped GQDs, including N-doped GQDs [18], P-doped GQDs [19], B-doped GQDs [20] and Si-doped GQDs [21] were synthesized successfully by our group. It has been proven that the as-prepared carbon quantum dots can possess strong fluorescence, low toxicity and excellent biolabeling to human Hela cells [18–20]. Based on these doped GQDs, multifunctional fluorescence sensing platforms for selective detection of Ag(I), Fe(III) and hydrogen peroxide, glucose and melamine were constructed and the results showed that the proposed detection platform may have great potential for quantitatively monitoring the intracellular species. Recently, we took advantage of high-performance fluorescence of GQDs and fluorescence resonance energy transfer (FRET) between GQDs and MWCNTs to build DNA sensors, which successfully achieved highly sensitive and selective analysis of the target DNA [22].

In the present study, we report the respective and simultaneous detection of DNA and bovine α-thrombin (thrombin) with high sensitivity and selectivity based on biocompatible GQDs and GO by taking advantage of the intense dual-color fluorescence of GQDs, efficient quenching effect of GO, specific recognition between probes and targets, and unique interaction between GQDs and GO. Dual-color GQDs were employed to synthesize blue and yellow probes for the recognition of target DNA and thrombin, respectively. As-prepared probes were placed on a GO platform, which acts separately as a quencher in order to achieve respective detection of DNA and thrombin. To realize simultaneous determination of DNA and thrombin, two GQD-labeled probes were assembled on the GO surface at the same time. By the integration of their specific interactions, the multifunctional nanosensor assembled with GO and two probes succeeded for convenient and simultaneous detection of DNA and thrombin through two on-off-on cycles of fluorescence for the first time.

2. Experimental

2.1. Materials and reagents

Triple-distilled water was used throughout the experimental process and to prepare PBS buffers. Graphite powder, sodium

borohydride, tetrahydrofuran, 1, 2-ethylenediamine, thionyl dichloride, 1-ethyl-3-(3-dimethylaminopropyl) carbodiimide hydrochloride (EDC · HCl) and N-hydroxylsuccinimide sodium salt (NHS) were purchased from Aladdin Ltd. (Shanghai, China). Bovine α-Thrombin was bought from Sigma (USA). Bovine serum albumin (BSA) and human IgG antibody were ordered from Shanghai Sangon Biotechnology Co. Ltd. (Shanghai, China). Phosphate buffer solution (PBS) was prepared by mixing stock solutions of NaH_2PO_4 and Na_2HPO_4. All reagents were of analytical grade and without any further purification. Thrombin apatamer (TA) and DNA oligonuleotides were purchased from Shanghai Sangon Biotechnology Co. Ltd. (Shanghai, China). Their sequences are listed as follows:

Capturing ssDNA sequence:

5'-COOH-CTG ATT ACT ATT GCA TGA GGC CTT-3';

Target ssDNA sequence (tDNA: perfectly matched with capturing ssDNA):

5'-AAG GCC TCA TGC AAT AGT AAT CAG-3';

Single-base mismatched ssDNA sequence (mDNA-1):

5'-AAG GCC TCA TGC AAT A**T**T AAT CAG-3';

Several-base mismatched ssDNA sequence (mDNA-2):

5'-CCT CAT **CGT TCG C**TT **CTC CAA**-3';

Thrombin aptamer sequence (TA):

5'-TCT CTC AGT CCG TGG TAG GGC AGG TTG GGG TGA CT-3'.

2.2. Synthesis of graphene oxide (GO).

GO was synthesized from graphite powder based on a modified Hummer's method according to literature. Briefly, graphite powder (1.0 g) was added to 33 mL of cold sulfuric acid (0 °C), where $KMnO_4$ (6.0 g) was slowly added under continuous stirring in ice-bath. After 15 min, $NaNO_3$ (1.0 g) was added into the mixture. The solution was further stirred for 1.5 h at 35 °C and then an amount of distilled water (40 mL) was added. Then the temperature was increased to 95 °C and the reaction was allowed for 35 min. In the end, the reaction was stopped with the addition of a mixture of 100 mL of distilled water and 6 mL of H_2O_2 (30%). The obtained golden dispersion was finally subjected to centrifugation at 1000 r.p.m. for 5 min to unexfoliated GO. The resulting supernatant solution was washed by distilled water and then subjected to centrifugation at 4000 r.p.m until the solution is neutral.

2.3. Synthesis of pristine graphene quantum dots (GQDs)

Graphite powder (0.3 g) was added into a mixture of concentrated sulfuric acid (180 mL) and nitric acid (60 mL). The solution was sonicated for two hours and heated at 80 °C for 24 h. The mixture was cooled and diluted with deionized water (800 mL). The dark brown GQD solution was neutralized with sodium carbonate. The final product solution was further dialyzed in a dialysis bag (1000 Da) for 3 d.

2.4. Synthesis of 1, 2-ethylenediamine functionalized graphene quantum dots (eGQDs) and chemically reduced graphene quantum dots (rGQDs)

The preparation of eGQDs was described in our previous paper in detail [17]. Briefly, a mixture of as-prepared GQDs (0.1 g) and $SOCl_2$ (20 mL) was reacted for 2 h at 80 °C, and then vacuum distillation was carried out to remove excessive $SOCl_2$. Twenty mL of 1, 2-ethylenediamine was added into the chlorinated GQDs and the mixture was heated at 100 °C for 4 h. The excessive 1, 2-ethylenediamine of the resulting mixture was removed by vacuum distillation, and the residue was washed with ethanol several times. For the synthesis of rGQDs, 1.6 g of GQDs and excessive sodium borohydride were added into 20 mL of tetrahydrofunan. The reaction was allowed for 8 h at 70 °C with gentle stirring. The solvent THF was removed by vacuum distillation and the residue was washed with ethanol several times. Finally, the as-prepared mixture was dialyzed using a dialysis bag (1000 Da).

2.5. Preparation of the ssDNA-eGQDs probe and TA-rGQDs probe

The obtained eGQDs were first dissolved in 10.0 mL of PBS solution (10 mM, pH 7.4), and then 1-ethyl-3-(3-dimethylaminopropyl)-carbodiimide (EDC) (80.0 mg) and N-hydroxysulfosuccinimide sodium salt (sulfo-NHS) (80.0 mg) were added to the resulting solution at room temperature with continuous stirring. After 30 min' activation, capturing ssDNA (15 μL, 100.0 nM) was added into the resulting solution. The condensation reaction was allowed for 24 h at room temperature with stirring. The DNA probes were then obtained by centrifugation and washing with a PBS buffer. For the preparation of the TA-rGQDs probe, the as-prepared rGQDs were first dissolved in 5.0 mL of phosphate buffer (10 mM, pH 7.0), and then the solution was adjusted to pH 5 with dilute hydrochloric acid for protonation of carboxyl groups of rGQDs. After that, 80.0 mg of EDC and 80.0 mg of sulfo-NHS were added into the resulting solution in order to activate the carboxylic group of rGQDs for 30 min at room temperature with stirring. 20.0 μL (100.0 μM) of thrombin aptamer was subsequently added into the above solution, and the reaction was allowed to process for 24 h. Finally, a TA-rGQDs probe was attained by centrifugation and washing with a PBS buffer.

2.6. Separate detection of DNA and thrombin based on an assembled nanosensor with GQDs and GO.

Optimum conditions including the amount of added GO, as well as equilibrium time for quenching and recovery, were optimized for DNA and thrombin detection respectively using the following procedure. (1) Amount of added GO: 3.0 mL of ssDNA-eGQDs probe or TA-rGQDs probe suspension in PBS buffer solution was prepared, and then a series of GO solutions with different concentrations was added into the resulting solution, which was finally diluted to 4.0 mL with the buffer solution. The fluorescence intensity of the mixed solution was determined using a fluorescence spectrometer

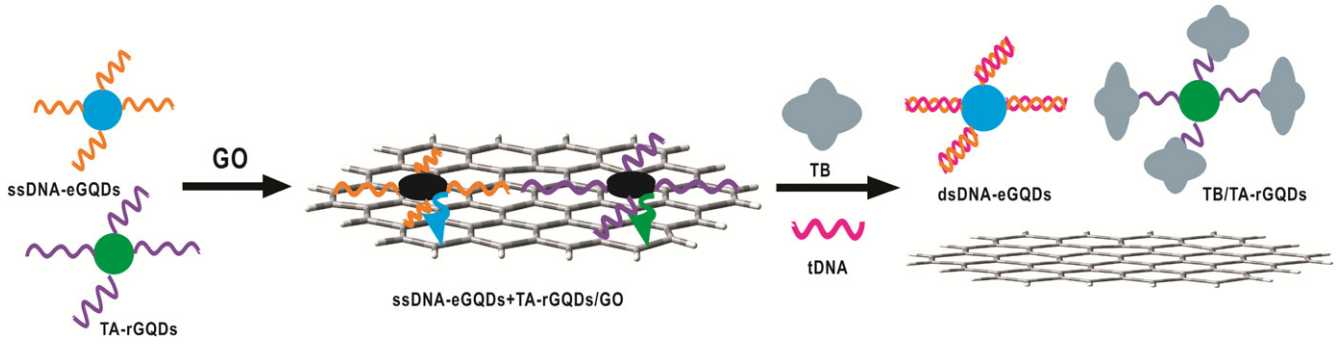

Scheme 1. Schematic illustration of dual-species detection strategy through self-assembly and self-recognition among GQD-labeled probes, GO and targets.

after a certain amount of incubation time. (2) Equilibrium time for quenching: a certain amount of GO solution was added into 3.0 mL of ssDNA-eGQDs probe or TA-rGQDs probe suspension. The resulting solution was finally diluted to 4.0 mL with the buffer solution and incubated in the incubator shaker. The fluorescence intensity of the mixed solution at different incubation times was recorded. (3) Equilibrium time for fluorescence recovery: a certain amount of GO solution and 2.0 μL of tDNA or thrombin was added into 3.0 mL of ssDNA-eGQDs probe or TA-rGQDs probe suspension. The resulting solution was finally diluted to 4.0 mL with the buffer solution and incubated in the incubator shaker. The fluorescence intensity of the mixed solution at different incubation time was recorded.

Under optimum conditions, respective detection of DNA and thrombin was performed respectively using the similar procedure as follows: 3.0 mL of ssDNA-eGQDs or TA-rGQDs probe suspension in buffer solution was prepared, and then a certain amount of GO (9.0 and 15.5 μg mL^{-1} GO for DNA and thrombin detection respectively) was introduced into the resulting solution at room temperature to initiate the quenching reaction. After 2 min of incubation, different concentrations of target DNA or thrombin were added into the solution, and the resulting solutions were finally diluted to 4.0 mL. After a certain time of incubation (20 and 60 min for DNA and thrombin detection respectively) at room temperature, the fluorescence intensity of the mixed solutions was measured under their optimal excitation wavelength.

2.7. Simultaneous detection of DNA and thrombin

10.0 μL of ssDNA-eGQDs probe and 100.0 μL of the TA-rGQDs probe were mixed, and then the mixture was diluted with PBS to a volume of 500.0 μL. 6.0 μL of GO (1.2 mg mL^{-1}) was introduced into the resulting mixture at room temperature in order to quench fluorescence with 10 min of incubation. Then, different concentrations of target DNA were added into the above solution to initiate the fluorescence recovery. After incubation for 60 min at room temperature, the fluorescence intensity of the resulting solutions was measured using synchronous fluorescence ranging from 250 to 600 nm with the constant value of the $\Delta\lambda = 76$ nm. Furthermore, various concentrations of thrombin were added into the resulting systems, and after 60 min' incubation, the fluorescence intensity of the mixed solutions was determined using synchronous fluorescence with the same parameter setting.

2.8. Characterization methods

The morphologies of all samples were characterized by transmission electron microscopy (TEM), which was performed on a JEOL-2100F instrument with an accelerating voltage of 200 kV. Samples were prepared by dropping aqueous suspensions of the separated fractions of samples onto Cu TEM grids coated with a holey amorphous carbon film, followed by solvent evaporation in a dust protected atmosphere. The x-ray photoelectron spectroscopy analyses were conducted using a Kratos Axis ULTRA x-ray photoelectron spectrometer with a 165 nm hemispherical electron energy analyzer. The incident radiation came from monochromatic Al x-ray (1486.6 eV) at 15 kV and 3 mA. Wide survey scans were taken at an analyzer pass energy of 160 eV over a 1400–0 eV binding energy with 1.0 eV step and a dwell time of 100 ms, while narrow multiplex higher resolution scans were performed at a pass energy of 20 eV with 0.05 eV step and a dwell time of 200 ms. The pressure in the analysis chamber was less than 7.5×10^{-9} Torr during sample analysis. Atomic concentrations were calculated using Vision software and a Shirley baseline. The UV–Vis spectra were recorded on a Perkin Elmer Lambda 950 spectrometer, in which the sample was dispersed in water after ultrasonication for 30 min The photoluminescence spectra were conducted on a PerkinElmer LS-55 fluorescence spectrometer, and lifetimes were determined using a FLS920 fluorescence spectrophotometer.

3. Results and discussion

3.1. Principle of separate and simultaneous detection for DNA and thrombin based on GQDs and GO

Good biocompatibility, high quantum yields, multiple fluorescence colors and excellent photostability make GQDs the best choice as fluorophores in biosensors. Although multiple colored GQDs including blue, green and yellow have been reported, suitable GQDs whose fluorescence emission

remains non-shifted and separates apparently from others' emission are still not easy to prepare in a large scale because most GQDs possess excitation wavelength dependence emissions [23–26]. In this case, we prepared two non-shifted GQDs with blue and green fluorescence as fluorophores of the following probes. GO has been used as a good electron acceptor and effective quencher to build chemosensors and biosensors, and thus was chosen as the platform and quencher in this work. DNA and thrombin as two distinct biomarkers are designated as representative detection targets in this study.

Scheme 1 displays the schematic illustration of the dual-species detection strategy based on electron transfer between GQD-labeled probes and GO. Pristine GQDs from the oxidation of graphite with mixed acids have quite weak green fluorescence with a quantum yield of 0.017 [17]. To better promote the sensitivity of as-constructed nanosensors, 1, 2-ethylenediamine-functionalized GQDs (eGQDs) and reduced GQDs (rGQDs) with high quantum yields (0.176 and 0.204) and different emission bands were prepared respectively. By employing the condensation reaction with EDC, eGQDs and capturing DNA (cDNA) were used to synthesize the DNA probe denoted as ssDNA-eGQDs, while rGQDs and thrombin-aptamer (TA) were adopted to prepare thrombin probe denoted as TA-rGQDs. Separate detections of DNA and thrombin are accomplished in a similar procedure: in the first step, either the ssDNA-eGQDs probe or the TA-rGQDs probe is mixed with GO so that the probe can adsorb on the surface of GO through electrostatic attraction and π–π stacking interaction, where either the assembly ssDNA-eGQDs/GO or TA-rGQDs/GO forms. The formation of the corresponding assembly leads to substantial fluorescence quenching of the original probe through electron transfer between probes and GO. It has been proven that efficient electron transfer between GQDs and GO occurs and subsequently leads to effective fluorescence quenching of GQDs [27]. In the second step, upon the addition of tDNA, tDNA can hybridize with ssDNA-eGQDs in the assembly ssDNA-eGQDs/GO to produce dsDNA-eGQDs through specific base pairing. The formation of dsDNA-eGQDs breaks up electrostatic attraction and the π–π stacking interaction between the probe and GO, and thus results in desorption of dsDNA-eGQDs from the surface of GO and subsequent fluorescence recovery from free dsDNA-eGQDs. On the other hand, in the second step in the detection of thrombin, the added thrombin can form a thrombin-aptamer complex with TA-rGQDs, i.e. TB/TA-rGQDs, because the aptamer specifically binds to thrombin exosite I by its TT loops through a mix of hydrophobic and polar interactions [28, 29]. The formation of TB/TA-rGQDs complex enables the liberation of the TA-rGQDs probe from the GO, and thus leads to apparent fluorescence recovery from this complex. To achieve the purpose of simultaneous detection of DNA and thrombin, the blue and yellow probes are assembled on the GO at the same time, and thus the assembled dual-functional nanosensor can synchronously respond to the presence of both DNA and thrombin due to the corresponding fluorescence enhancement induced by the freedom of their respective complex from the GO surface.

3.2. Synthesis and characterization of dual-colored probes

The pristine GQDs were used as the starting materials because they possess rich functionals including carboxylic acids and hydroxyl groups and are easy to prepare in large scale from oxidation of graphite with concentrated nitric and sulfuric acids. However, the pristine GQDs need further improvement in fluorescence emission efficiency because of their quite low quantum yield of 0.017. Two kinds of treatments including surface functionalization with 1, 2-ethylenediamine and chemical reduction with $NaBH_4$ were employed to greatly enhance the fluorescence of GQDs. Thus, highly fluorescent 1, 2-ethylenediamine-functionalized GQDs (eGQDs) and reduced GQDs (rGQDs) were obtained, respectively. According to our previous papers [17, 22], the quantum yields of eGQDs and rGQDs are up to 0.176 and 0.204, respectively, more than ten times of that of pristine GQDs. After the proceeding treatment, eGQDs possess a great deal of $–NH_2$ groups whereas rGQDs are rich in CO_2H groups. Using the similar condensation reaction with the same reagent 1-ethyl-3-(3-dimethylaminopropyl)-carbodiimide (EDC), eGQDs react with CO_2H-functionalized DNA (ssDNA) to form ssDNA-eGQDs probes bonded with the -CONH- group, whereas rGQDs bind with thrombin-aptamer (TA) to produce TA-rGQDs probes through the –COO- group.

The ssDNA-eGQDs and TA-rGQDs probes show similar size distribution of 3–5 nm with their respective GQDs because the sizes of both eGQDs and rGQDs fall in this range, as illustrated in our previous report [17, 22]. Figure S1 clearly verifies the size range of the two probes, showing their TEM images. eGQDs and rGQDs have the close central emission bands at their optimal excitation wavelength, but exhibit blue and bluish-green color respectively under the UV light. Figure 1 displayed normalized fluorescence spectra of all species involved in the detection route. The ssDNA-eGQDs probe shows intense fluorescence emission centered at 414 nm, while the TA-rGQDs probe strongly emits greenish-yellow light at around 506 nm, i.e. when they are excited by their own optimal excitation light. One can notice that the fluorescence spectrum of eGQDs largely overlaps that of rGQDs, but the eGQDs-labeled probe ssDNA-eGQDs separates well in fluorescence emission from the rGQDs-labeled probe TA-rGQDs. This good separation in their fluorescence emission is helpful for the subsequent accomplishment of simultaneous detection, and can be attributed to an inverse shift in fluorescence emission owing to the formation of different linking moieties (-CONH- or -COO-) between the GQDs and DNA sequence. The large shifts in emission between probes and their GQDs provide solid evidence for a successful binding link between GQDs and DNA sequence, i.e. successful synthesis of the probes. The fluorescence spectra of cDNA, tDNA, TA and TB were also shown in figure 1, but it should be emphasized that these species have quite weak fluorescence, and thus their contribution in the fluorescence of the probes is negligible relative to those of the GQDs. The distinct time-resolved decay curves between probes and respective GQDs shown in figure

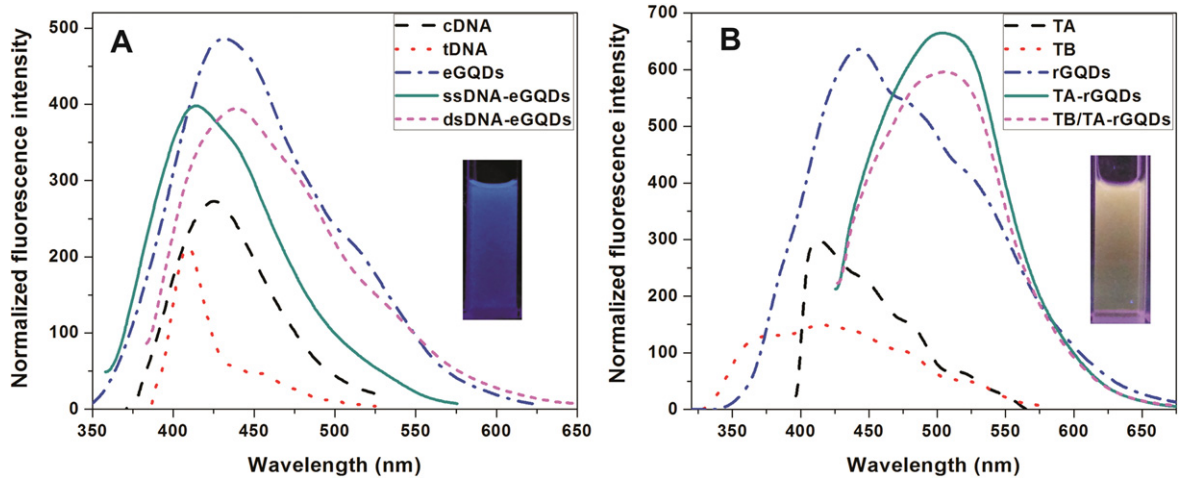

Figure 1. (A) The fluorescence spectra of cDNA, tDNA, eGQDs, ssDNA-eGQDs, dsDNA-eGQDs. (B) The fluorescence spectra of TA, TB, rGQDs, TA-rGQDs, TB/TA-rGQDs. Inset: the fluorescence images of ssDNA-eGQDs and TA-rGQDs probes.

Table 1. The fluorescence parameters of ssDNA-eGQDs, TA-rGQDs and their respective GQDs.

	λ_{ex}^{a} (nm)	λ_{em}^{b} (nm)	ϕ^{c} (%)	τ^{d} (ns)
eGQDs	355	440	17.6	5.7
ssDNA-eGQDs	340	416	15.9	4.0
rGQDs	351	443	20.4	2.1
TA-rGQDs	400	506	18.2[e]	3.4

[a] Optimal excitation wavelength.
[b] Optimal emission wavelength.
[c] Quantum yield determined relative to quinine sulfate.
[d] Lifetime.
[e] Quantum yield determined using Rodanmine B as standard.

S2 further prove the attachment of the DNA sequence to the GQDs through chemical bonds. Table 1 summarizes the fluorescence parameters including optimal excitation and emission wavelength, lifetime and quantum yield of highly fluorescent species. It should be noted that high quantum yields of probes have been attained due to high emission efficiency from rGQDs or eGQDs with respect to pristine GQDs, which guarantees the high sensitivity of the following assembled sensors.

3.3. Respective detection of DNA and thrombin based on separate probe on a GO platform

In order to assess the respective detection of DNA and thrombin, ssDNA-eGQDs or TA-rGQDs were assembled on the GO surface in order to construct separate DNA sensor and thrombin aptasensor. For the DNA sensor, we first optimized the amount of added GO for quenching, fluorescence quenching time and recovery time. Figure S3 shows that the fluorescence intensity gradually decreases with the addition of GO, and nearly complete quenching is reached when the amount of GO is up to 9.0 μg mL^{-1}. Time dependence of fluorescence quenching of the probe with the addition of GO and subsequent fluorescence recovery with introduction of tDNA displayed in figure S4 indicates that fluorescence quenching reaches equilibrium in as short as 2 min, whereas fluorescence recovery with tDNA remains stable after 20 min' mixing. Thus, 9.0 μg mL^{-1} of GO, 2 min' quenching and 20 min' recovery were selected as the optimal conditions for the following detection of tDNA. The sensing performance of this nanosensor was evaluated by adding various concentrations of tDNA into the ssDNA-eGQDs/GO system. Figure 2 illustrates that the fluorescence intensity is gradually increased with the continuous addition of tDNA, and the fluorescence intensity shows a linear relationship with the concentration of tDNA. The linear fitting equation can be expressed as $y = 2.59x + 125.5$, where $R^2 = 0.993$. The established method has a broad detection range of 1.5–100.0 nM with a detection limit of 0.3 nM as estimated from the derived calibration curve (⩾3 standard deviations). These parameters are quite close to those reported in our previous papers [22]. The detection limit is comparable with those of DNA sensors based on dye-labeled probes and GO (0.1–1 nM) [5, 6, 9]. It should be noted that an apparent red-shift in emission of dsDNA-eGQDs can be observed with respect to ssDNA-eGQDs as shown in figure 1(A), which presents the proof for the formation of dsDNA-eGQDs.

For the thrombin aptasensor, optimal conditions were also assessed as with the DNA sensor. According to figures. S5 and S6, 15.5 μg mL^{-1} of GO, 2 min' quenching time and 60 min' recovery time were chosen as optimal conditions. One can notice that the thrombin sensor needs much more time to reach stable fluorescence recovery than the DNA sensor, which can be explained by the slow motion of thrombin and hard connection between thrombin and its aptamer. Under the same conditions, this nanosensor was assessed by monitoring fluorescence intensity change while increasing the concentration of thrombin into TA-rGQDs/GO system. Figure 3(A) demonstrates the gradual change in fluorescence intensity dependent on the concentration of thrombin. Upon the addition of 60.0 nM of thrombin, the fluorescence intensity is recovered to its original value before quenching. In figure 3(B) the fluorescence intensity shows a linear relationship with the concentration of thrombin in the range of 1.0–30.0 nM, where the fitting equation is described

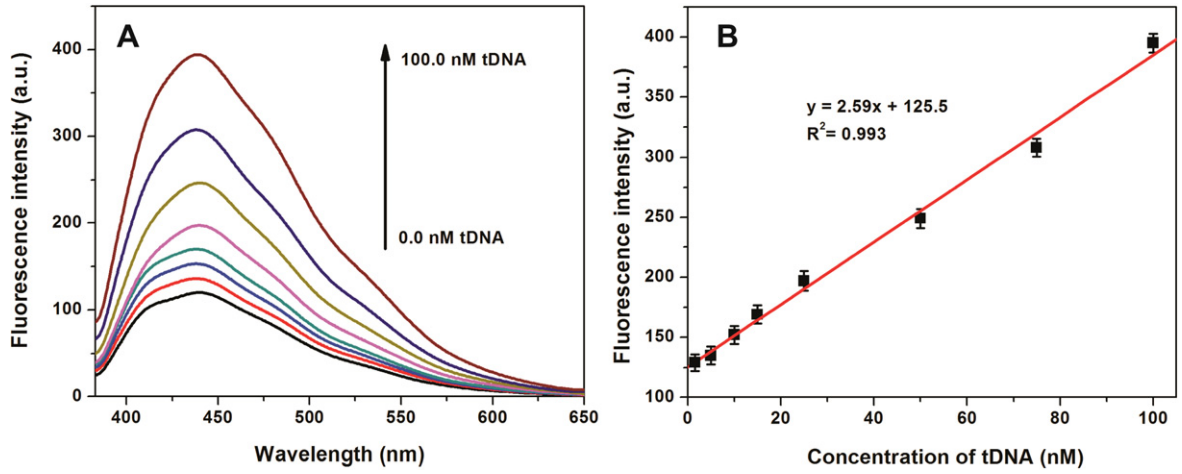

Figure 2. (A) The fluorescence recovery of ssDNA-eGQDs/GO system after incubation with various concentrations of tDNA (5.0, 10.0, 15.0, 25.0, 50.0, 75.0, 100.0 nM). (B) The linear relationship between the fluorescence intensity and concentration of tDNA.

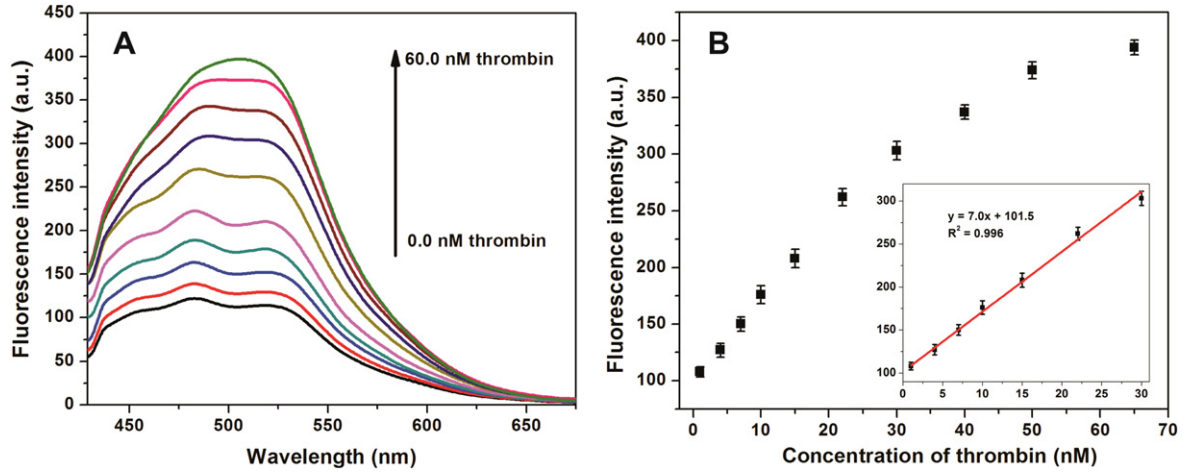

Figure 3. (A) The fluorescence recovery of TA-rGQDs/GO system after incubation with various concentrations of thrombin (4.0, 7.0, 10.0, 15.0, 22.0, 30.0, 40.0, 50.0, 60.0 nM). (B) The linear relationship between the fluorescence intensity and concentration of thrombin.

as $y = 7.0x + 101.5$ and $R^2 = 0.996$. Its detection limit was also estimated as 0.6 nM using the same methods as the DNA sensor, which is comparable with those of the aptasensors based on dye-labeled TA on mesoporous carbon microparticles (0.25 nM) [6], poly(m-phenylenediamine) (0.1 nM) [30], and single-walled carbon nanotubes (1.8 nM) [3]. It is also quite close to the detection limit of thrombin (0.5 nM) based on AgNP-labeled probe on GO reported recently [9].

To assess the selectivity of the DNA sensor and thrombin aptasensor, perfect matched tDNA, single base mismatched mDNA-1 and more than one base mismatched mDNA-2 were selected to compare with the DNA sensor, while thrombin, bovine serum albumin (BSA) and Immunoglobulin G (IgG) were chosen for the thrombin aptasensor. Figure 4(A) shows a much higher selectivity efficiency to tDNA than mDNA-1 with only single mismatched base, and a very weak response to mDNA-2. In our previous paper [22], we also tested mDNAs with two and three mismatched bases, and the results showed that they had nearly no response to DNA sensor, suggesting their good selectivity for DNA detection. Figure 4(B) illustrates that thrombin aptasensors are greatly selective to thrombin with respect to other proteins; selectivity efficiency to thrombin is up to 10 while no obvious response to BSA and IgG can be observed. The selectivity efficiency of this aptasensor is much higher than those based on dye-labeled probes (around 3) [3, 31, 32].

3.4. Simultaneous detection of DNA and thrombin based on dual probes on a GO platform

A dual-functional biosensor based on two-colored probes and GO was further constructed to explore simultaneous detection of DNA and thrombin. Although two probes possess distinct fluorescence colors, and have a large gap in maximum emission peak (up to 90 nm), they still cannot be distinguished from each other when mixed, as shown in figure S7, because both of them have a quite broad full width at half maximum (90 and 110 nm, respectively). To overcome this problem, we used synchronous fluorescence spectroscopy to differentiate their respective emissions. The comparison between normal and synchronous fluorescence in figure S7 displayed that synchronous spectroscopy has the ability to

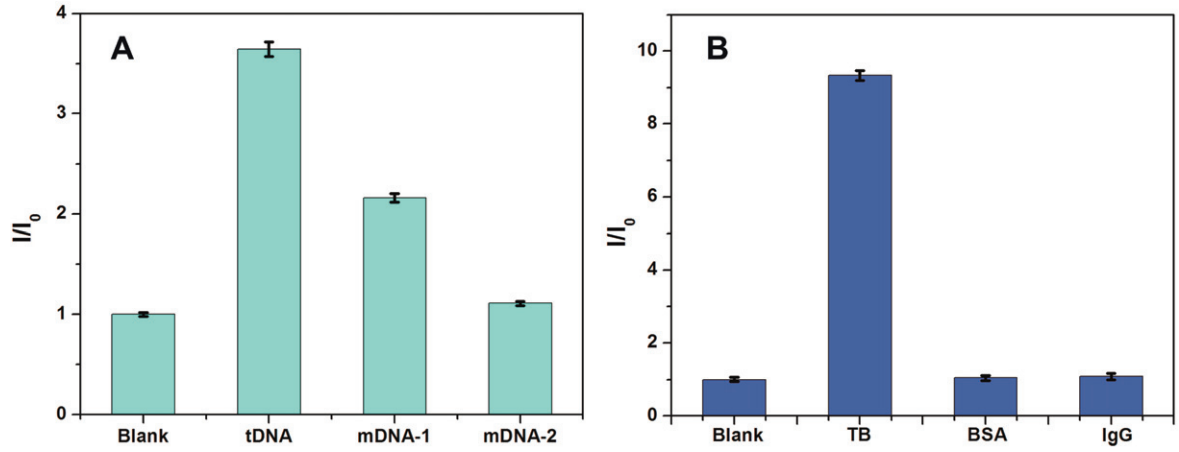

Figure 4. (A) Fluorescence intensity changes (I/I_0) of the aptasensor incubated in blank buffer, 100 nM of tDNA, mDNA-1 and mDNA-2 in buffer. Excitation was at 340 nm, and emission was monitored at 416 nm. (B) Fluorescence intensity changes (I/I_0) of the aptasensor incubated in blank buffer, 100 nM of TB, BSA and IgG in buffer. Excitation was at 400 nm, and emission was monitored at 506 nm.

identify the two probes, owing to its effectiveness in narrowing peak width, while no apparent distinction can be observed in the normal spectrum. The two probes show apparently distinct fluorescence emission peaks at 354 and 428 nm respectively with a $\Delta\lambda$ of 76 nm in the synchronous spectra, which enables simultaneous detection of DNA and thrombin. After the addition of 2.5 μg mL^{-1} of GO into the mixed probes system, the two probes were assembled onto the surface of the GO at the same time. The formation of the assembly (ssDNA-eGQDs+TA-rGQDs)/GO results in substantial fluorescence quenching due to electron transfer between the probes and GO. Figure S8 shows a similarly strong quenching effect of GO on both of the probes, and the presence of 2.5 μg mL^{-1} of GO leads to a reduction of more than 60% in intensity. The formation of the assembly (ssDNA-eGQDs+TA-rGQDs)/GO was also verified by the TEM images shown in figure 5. Figure 5(A) clearly demonstrates that a great deal of GQD-labeled probes are absorbed on the surface of GO as the assembly, and the high-resolution TEM image in figure 5(B) shows their similar size distribution and crystalline structure with their respective GQDs.

Compromising different conditions, 2.5 μg mL^{-1} of GO, 2 and 60 min' mixing for quenching and recovery were chosen to assess the performance of the dual-functional biosensor in quantitative analysis of DNA and thrombin at the same time. Figure 6(A) shows the gradual increase in fluorescence intensity of dsDNA-eGQDs with an increase in the concentration of tDNA up to 400 nM, while nearly no change in emission at 454 nm was observed for the thrombin probe. The fluorescence enhancement originates from the increase of fluorescent dsDNA-eGQDs due to the pairing between ssDNA-eGQDs and added tDNA. Figure 6(B) illustrates that the fluorescence intensity is linear with the concentration of tDNA from 22.2 to 400 nM; this equation can be expressed as $y = 0.45x + 254.4$ where $R^2 = 0.98$. Based the same method, its detection limit is estimated as 6.7 nM. One can notice that this detection limit is inferior to that for single detection of DNA, but its linear range up to 400.0 nM is much superior to that of the single detection method. After 400.0 nM of tDNA was added, various concentrations of thrombin were continuously introduced into this system. As shown in figure 7(A), the fluorescence intensity at 454 nm enhances step by step as we increase the concentration of thrombin until up to 1000.0 nM, whereas the fluorescence emission at 354 nm is not influenced by the addition of thrombin. As presented as the preceding section, this increase in fluorescence intensity comes from the TB/TA-rGQDs complex in increasing amounts, owing to selective recognition between the thrombin and its aptamer. Figure 7(B) shows its linear fitting curve with the equation of $y = 0.12x + 215.1$ and $R^2 = 0.99$. Its detection limit based on three standard errors is evaluated as 7.9 nM, which is also inferior to that for single detection of thrombin. This approach is much more advantageous in linear range from 79.0 to 1000.0 nM than that for single detection. In general, this dual-functional biosensor assembled with two probes and GO platform possesses the capability to simultaneously and quantitatively determine DNA and thrombin with a quite broad linear range and relatively low detection limit. Combining the advantages of the single detection and simultaneous detection approach, we can accomplish respective or simultaneous detection of dual species with high sensitivity, high selectivity and broad linear range.

4. Conclusion

The present study has introduced benign carbon-based materials to assemble multifunctional biosensors for respective and simultaneous detection of DNA and thrombin. Biocompatible GQDs were used as fluorophores in two-colored probes. High emission efficiency of GQDs guarantees high sensitivity of the constructed biosensors, and good biocompatibility provides promising opportunity for further utilization of the biosensors *in vivo*. Two-colored probes were synthesized by chemically attaching GQDs to the corresponding oligonucleotide sequence and thrombin aptamer targeting DNA and thrombin. The fluorescence of both of the

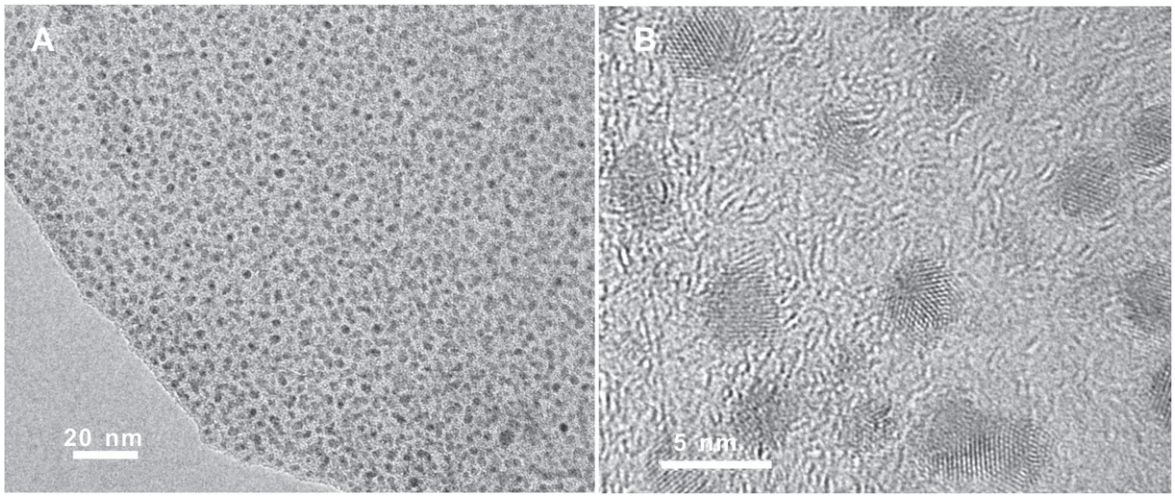

Figure 5. (A) TEM image of the ssDNA-eGQDs probe and TA-rGQDs probe on a GO surface. (B) High-resolution TEM of the GQDs-labeled probes.

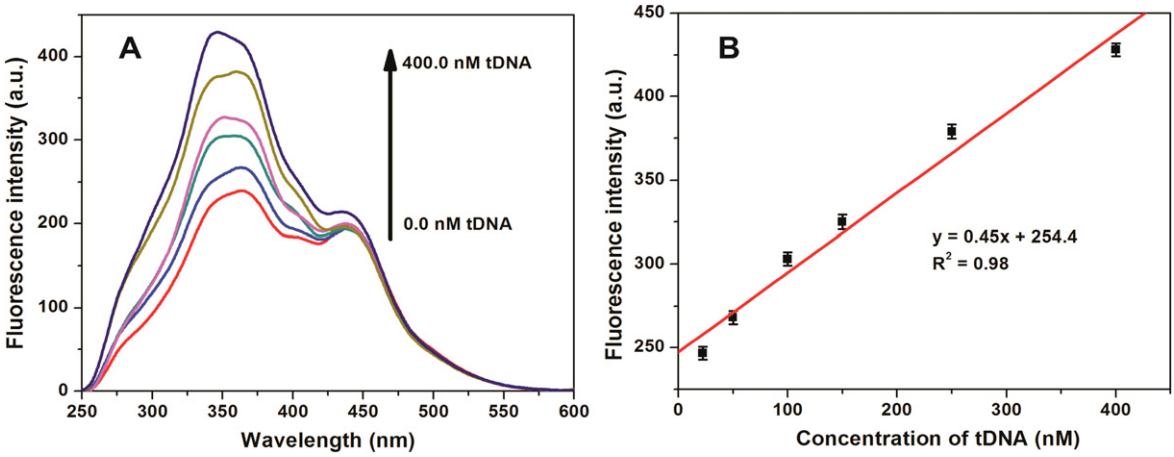

Figure 6. (A) The fluorescence recovery of mixed probes/GO system after incubation with various concentrations of tDNA (22.3, 50.0, 100.0, 150.0, 250.0, 400.0 nM). (B) The linear relationship between the fluorescence intensity and concentration of tDNA.

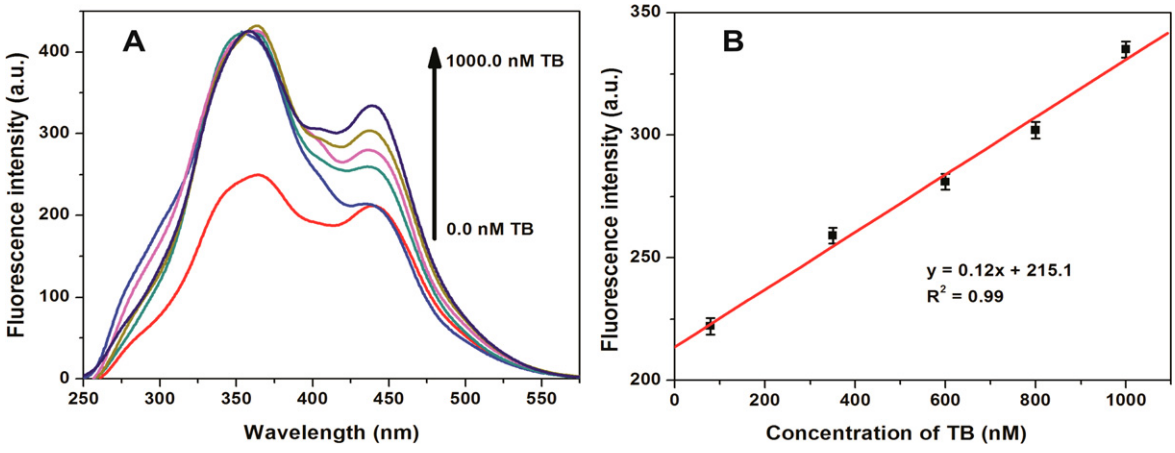

Figure 7. (A) The fluorescence recovery of a mixed probe/GO system after incubation with various concentrations of thrombin (79.0, 350.0, 600.0, 800.0, 1000.0 nM). (B) The linear relationship between the fluorescence intensity and concentration of thrombin.

probes can be efficiently quenched by GO through electron transfer between their assembly due to the specific π–π stacking and electrostatic attraction. The unique pairing between hybridized DNA pairs and distinctive recognition between thrombin and its aptamer result in the subsequent fluorescence recovery at the presence of DNA and/or thrombin. This fluorescence on-off-on process enables qualitative and quantitative analysis of DNA and thrombin. The two-colored probes labeled with GQDs not only can be absorbed separately on a GO platform to realize respective detection of DNA and thrombin, but also can be assembled on GO at the same time to achieve simultaneous analysis. Combining their respective advantages, separate and simultaneous detection of DNA and thrombin with super sensitivity, high selectivity and broad linear range can be accomplished. This dual-functional detection strategy can be served as a general approach for simultaneous detection of multiple biomolecules.

Acknowledgments

We are grateful for the support from the National Natural Science Foundation of China (No. 21405142, 21005073, 21275131), Zhejiang Province (No. LY13B050001, LQ13B050002) and Open Research Fund of Top Key Discipline of Chemistry in Zhejiang Provincial Colleges and Key Laboratory of the Ministry of Education for Advanced Catalysis Materials (Zhejiang Normal University).

References

[1] Giljohann D A and Mirkin C A 2009 *Nature* **462** 461–4
[2] Xu H, Li Q, Wang L, He Y, Shi J, Tang B and Fan C 2014 *Chem. Soc. Rev.* **43** 2650–61
[3] Yang R, Tang Z, Yan J, Kang H, Kim Y, Zhu Z and Tan W 2008 *Anal. Chem.* **80** 7408–13
[4] Chen J, Huang Y, Shi M, Zhao S and Zhao Y 2013 *Talanta* **109** 160–6
[5] He S, Song B, Li D, Zhu C, Qi W, Wen Y, Wang L, Song S, Fang H and Fan C 2010 *Adv. Funct. Mater.* **20** 453–9
[6] Zhang M, Yin B C, Tan W and Ye B C 2011 *Biosens. Bioelectron.* **26** 3260–5
[7] Li N, Chang C, Pan W and Tang B 2012 *Angew, Chem. Int. Ed.* **51** 7426–30
[8] Mei Q and Zhang Z 2012 *Angew, Chem. Int. Ed.* **51** 5602–6
[9] Liu X, Wang F, Aizen R, Yehezkeli O and Willner I 2013 *J. Am. Chem. Soc.* **135** 11832–9
[10] Chen L, Zhang X, Zhou G, Xiang X, Ji X, Zheng Z, He Z and Wang H 2012 *Anal. Chem.* **84** 3200–7
[11] Zhang H, Zhang L, Liang R P, Huang J and Qiu J D 2013 *Anal. Chem.* **85** 10969–76
[12] Nagy A, Steinbru¨ck A, Gao J, Doggett N, Hollingsworth J A and Iyer R 2012 *ACS Nano* **6** 4748–62
[13] Choi S, Dickson R M and Yu J 2012 *Chem. Soc. Rev* **41** 1867–91
[14] Baker S N and Baker G A 2010 *Angew. Chem. Int. Ed.* **49** 6726–44
[15] Shen J, Zhu Y, Yang X and Li C 2012 *Chem. Commun.* **48** 3686–99
[16] Li H, Kang Z, Liu Y and Lee S-T 2012 *J. Mater. Chem.* **22** 24230–53
[17] Qian Z, Ma J, Shan X, Shao L, Zhou J, Chen J and Feng H 2013 *RSC Adv.* **3** 14571–9
[18] Qian Z, Ma J, Shan X, Feng H, Shao L and Chen J 2014 *Chem. Eur. J.* **20** 2254–63
[19] Zhou J, Shan X, Ma J, Gu Y, Qian Z, Chen J and Feng H 2014 *RSC Adv.* **4** 5465–8
[20] Shan X, Chai L, Ma J, Qian Z, Chen J and Feng H 2014 *Analyst* **139** 2322–5
[21] Qian Z, Shan X, Chai L, Ma J, Chen J and Feng H 2014 *ACS Appl. Mater. Interfaces.* **6** 6797–805
[22] Qian Z S, Shan X Y, Chai L J, Ma J J, Chen J R and Feng H 2014 *Biosens. Bioelectron.* **60** 64–70
[23] Sun Y-P *et al* 2006 *J. Am. Chem. Soc.* **128** 7756–7
[24] Liu H, Ye T and Mao C 2007 *Angew. Chem. Int. Ed.* **46** 6473–5
[25] Li H, He X, Kang Z, Huang H, Liu Y, Liu J, Lian S, Tsang C H, Yang X and Lee S T 2010 *Angew. Chem. Int. Ed.* **49** 4430–4
[26] Peng J *et al* 2012 *Nano Lett.* **12** 844–9
[27] Yu P, Wen X, Toh Y-R, Lee Y-C, Huang K-Y, Huang S, Shrestha S, Conibeer G and Tang J 2014 *J. Mater. Chem.* C **2** 2894–901
[28] Russo Krauss I, Merlino A, Giancola C, Randazzo A, Mazzarella L and Sica F 2011 *Nucleic Acids Res.* **39** 7858–67
[29] Jiao F, Fan H, Yang G, Zhang F and He P 2013 *J. Mol. Recognit.* **26** 672–8
[30] Zhang Y and Sun X 2011 *Chem. Commun.* **47** 3927–9
[31] Zhang Y, Liu S and Sun X 2011 *Biosens. Bioelectron.* **26** 3876–80
[32] Chang H, Tang L, Wang Y, Jiang J and Li J 2010 *Anal. Chem.* **82** 2341–6